

Supplementary Materials for

A Novel Method for Quantifying the Contribution of Regional Transport to PM<sub>2.5</sub> in Beijing (2013-2020): Combining Machine Learning with Concentration-Weighted Trajectory Analysis

Kang Hu<sup>1</sup>, Hong Liao<sup>1</sup>, Dantong Liu<sup>2</sup>, Jianbing Jin<sup>1</sup>, Lei Chen<sup>1</sup>, Siyuan Li<sup>2</sup>, Yangzhou Wu<sup>3</sup>, Changhao Wu<sup>4</sup>, Shitong Zhao<sup>2</sup>, Xiaotong Jiang<sup>5</sup>, Ping Tian<sup>6,7</sup>, Kai Bi<sup>6,7</sup>, Ye Wang<sup>8</sup>, Delong Zhao<sup>6,7</sup>

<sup>1</sup>Jiangsu Collaborative Innovation Center of Atmospheric Environment and Equipment Technology, Jiangsu Key Laboratory of Atmospheric Environment Monitoring and Pollution Control, Nanjing University of Information Science & Technology, Nanjing 210044, China.

<sup>2</sup>Department of Atmospheric Sciences, School of Earth Sciences, Zhejiang University, Hangzhou 310058, China.

<sup>3</sup>Guangxi Key Laboratory of Environmental Pollution Control Theory and Technology, Guilin University of Technology, Guilin 541004, China.

<sup>4</sup>Institute of International Rivers and Eco-security, Yunnan University, Kunming 650091, China.

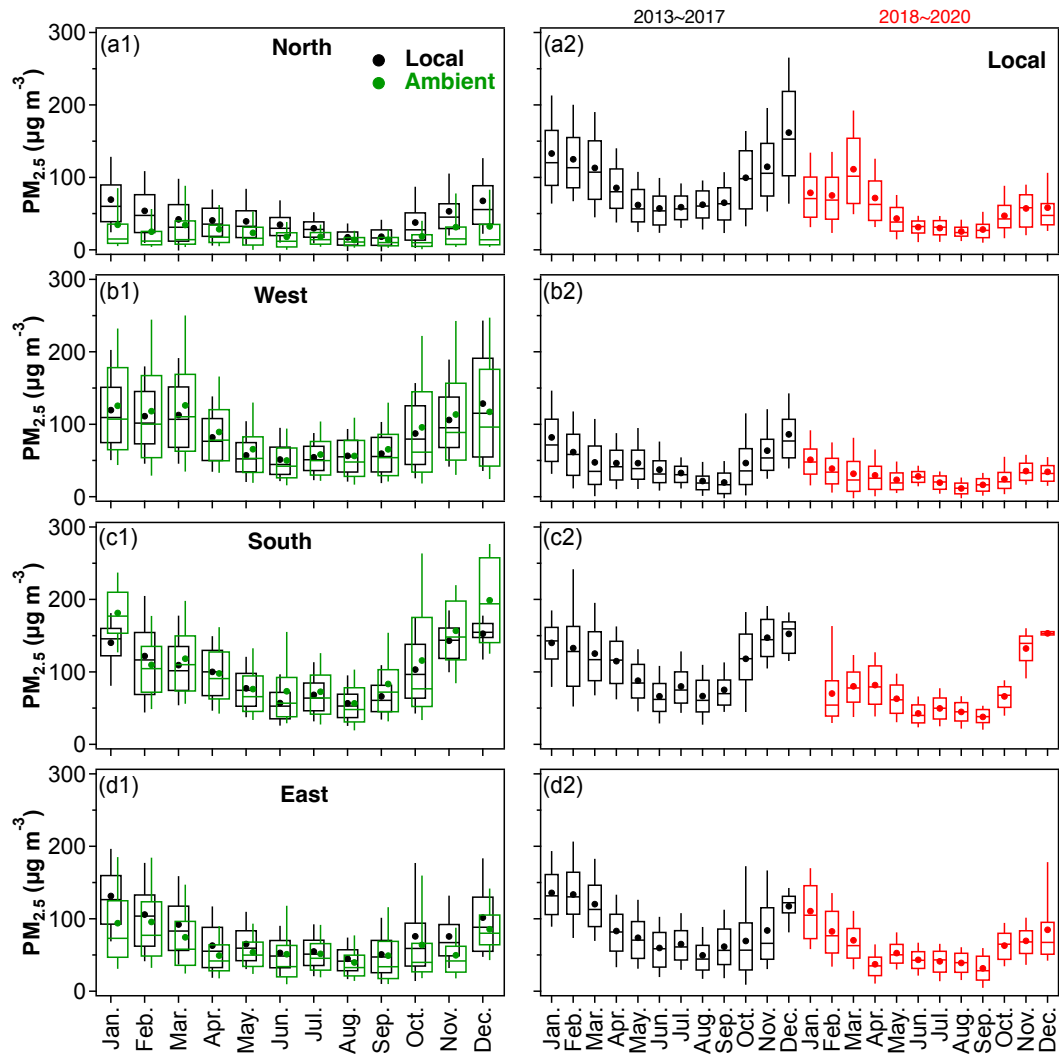
<sup>5</sup>College of Biological and Environmental Engineering, Shandong University of Aeronautics, Binzhou, 256600, China.

<sup>6</sup>Beijing Key Laboratory of Cloud, Precipitation and Atmospheric Water Resources, Beijing 100089, China.

<sup>7</sup>Field Experiment Base of Cloud and Precipitation Research in North China, China Meteorological Administration, Beijing 100089, China.

<sup>8</sup>Key Laboratory of Meteorological Disaster, Ministry of Education (KLME)/Joint International Research Laboratory of Climate and Environment Change (ILCEC)/ Collaborative Innovation Center on Forecast and Evaluation of Meteorological Disasters (CIC-FEMD), Nanjing University of Information Science and Technology, Nanjing 210044, China.

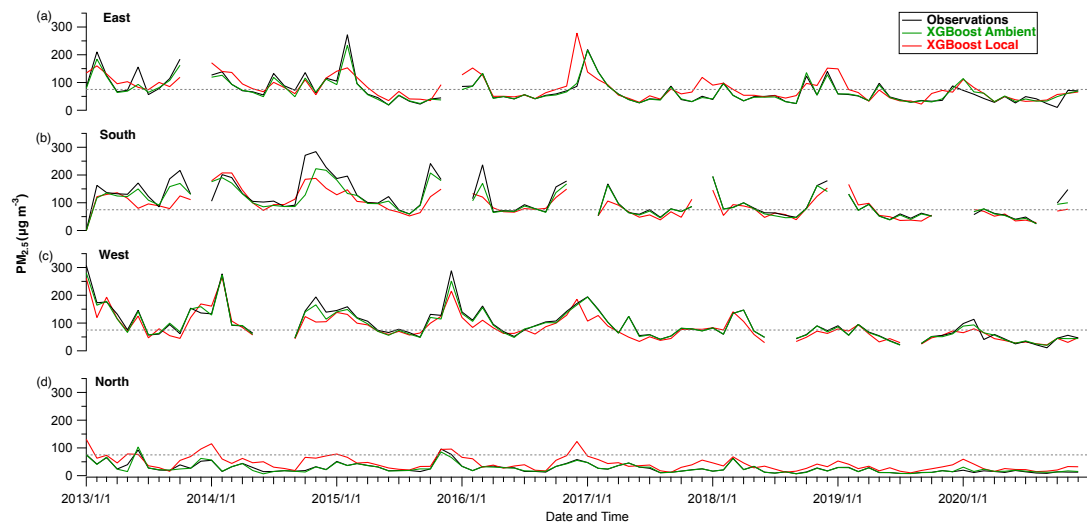
Corresponding author: Hong Liao ([hongliao@nuist.edu.cn](mailto:hongliao@nuist.edu.cn))



29

30 Fig. S1. Monthly variations of local (black) and ambient (green) PM<sub>2.5</sub> from the (a1) North, (b1)  
 31 West, (c1) South, and (d1) East regions during 2013-2020. Right panels show monthly  
 32 variations of local PM<sub>2.5</sub> before (black) and after (red) 2017 for the corresponding source  
 33 regions in the left panels. The upper and lower boundaries represent the 75<sup>th</sup> and 25<sup>th</sup> percentiles,  
 34 respectively, while the solid origin represents the average value.

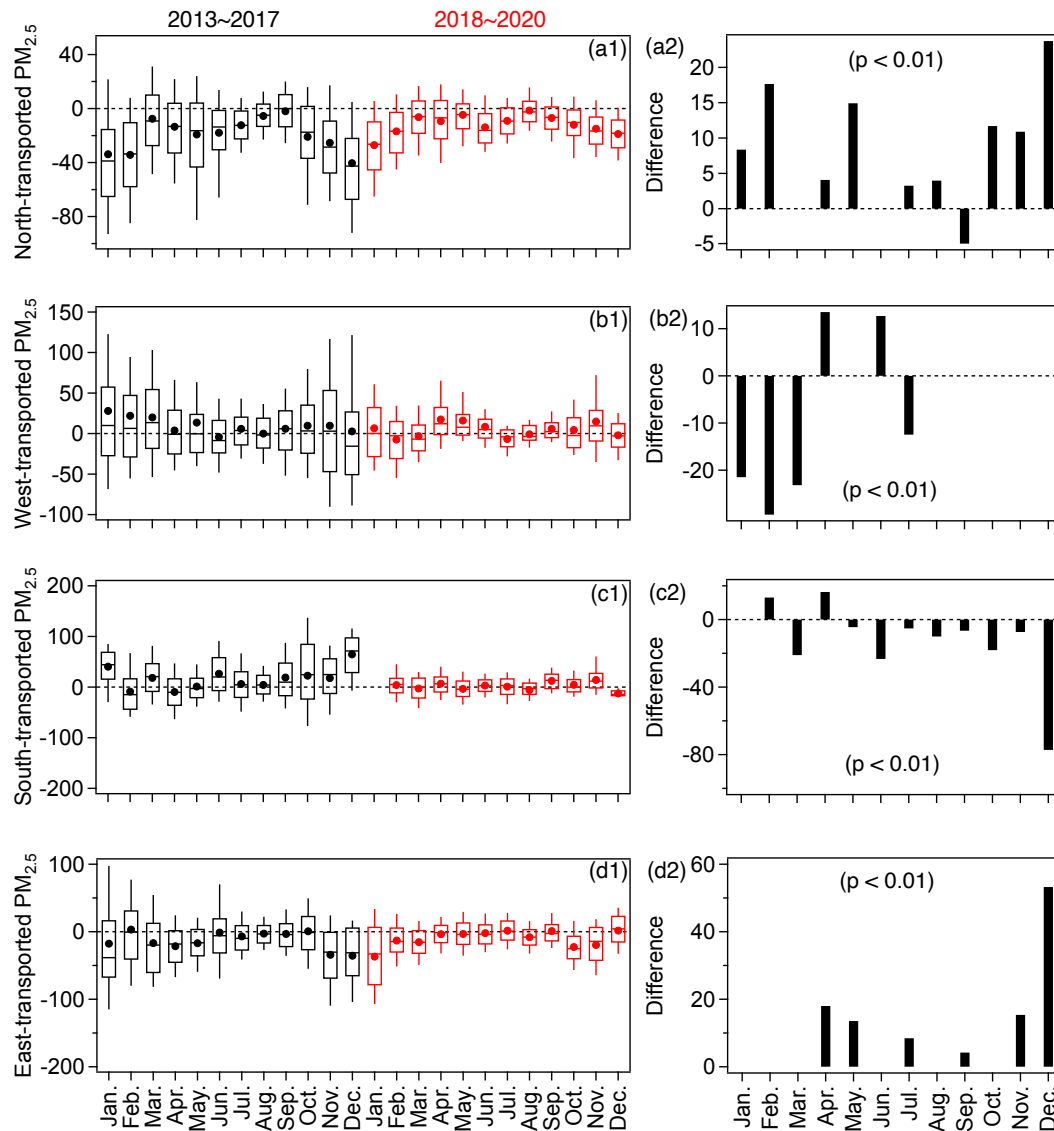
35



36

37 Fig. S2. Temporal variations of monthly PM<sub>2.5</sub> from the (a) East, (b) South, (c) West, and (d)  
 38 North regions. Black, green, and red lines represent observations, XGBoost model results for  
 39 ambient PM<sub>2.5</sub>, and local PM<sub>2.5</sub>, respectively. The horizontal dash line represents a PM<sub>2.5</sub>  
 40 concentration of 75 µg m<sup>-3</sup>.

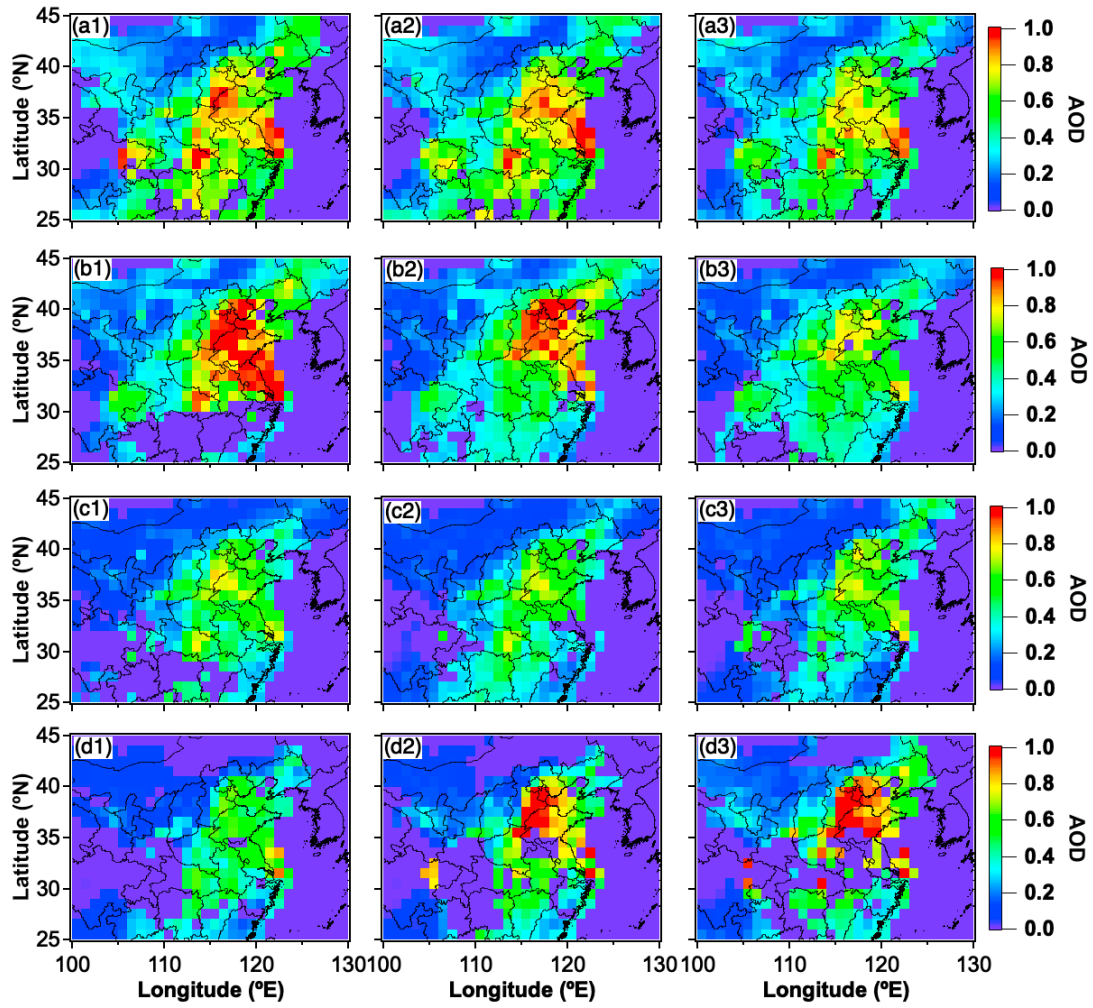
41



42

43 Fig. S3 Monthly variations of  $PM_{2.5}$  transmitted from the (a1) North, (b1) West, (c1) South, and  
 44 (d1) East regions during 2013-2017 (black) and 2018-2020 (red). The upper and lower  
 45 boundaries represent the 75<sup>th</sup> and 25<sup>th</sup> percentiles, respectively, while the solid origin represents  
 46 the average value. The right panels display the absolute change in monthly average differences  
 47 between the periods 2013-2017 and 2018-2020. Only results passing the  $t$ -test ( $p < 0.01$ ) are  
 48 shown.

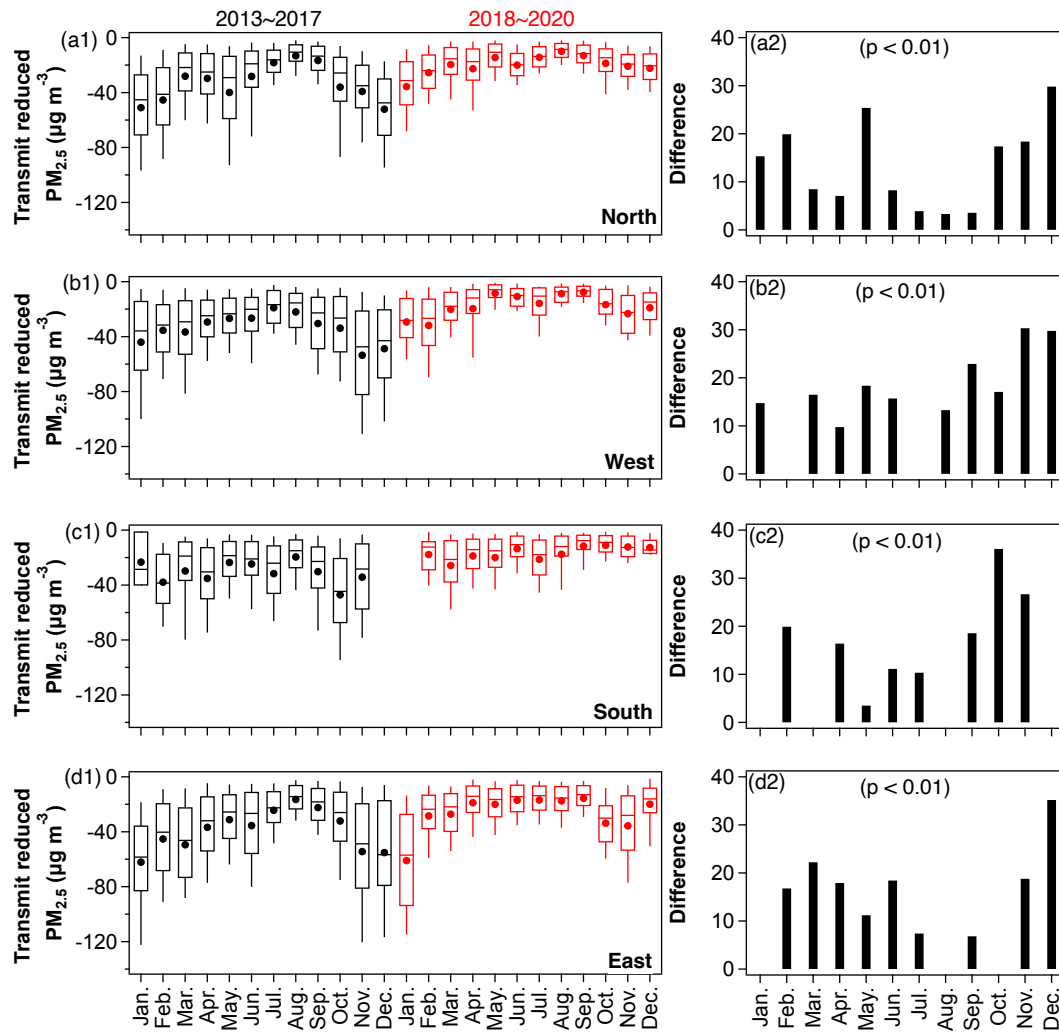
49



50

51 Fig. S4. Spatial climatology of monthly mean aerosol optical depth (AOD) at 550 nm based on  
 52 daily Collection 6 (C006) combined Dark Target and Deep Blue MODIS Aqua retrievals for  
 53 (a1) March, (a2) April, (a3) May, (b1) June, (b2) July, (b3) August, (c1) September, (c2)  
 54 October, (c3) November, (d1) December, (d2) January, and (d3) February.

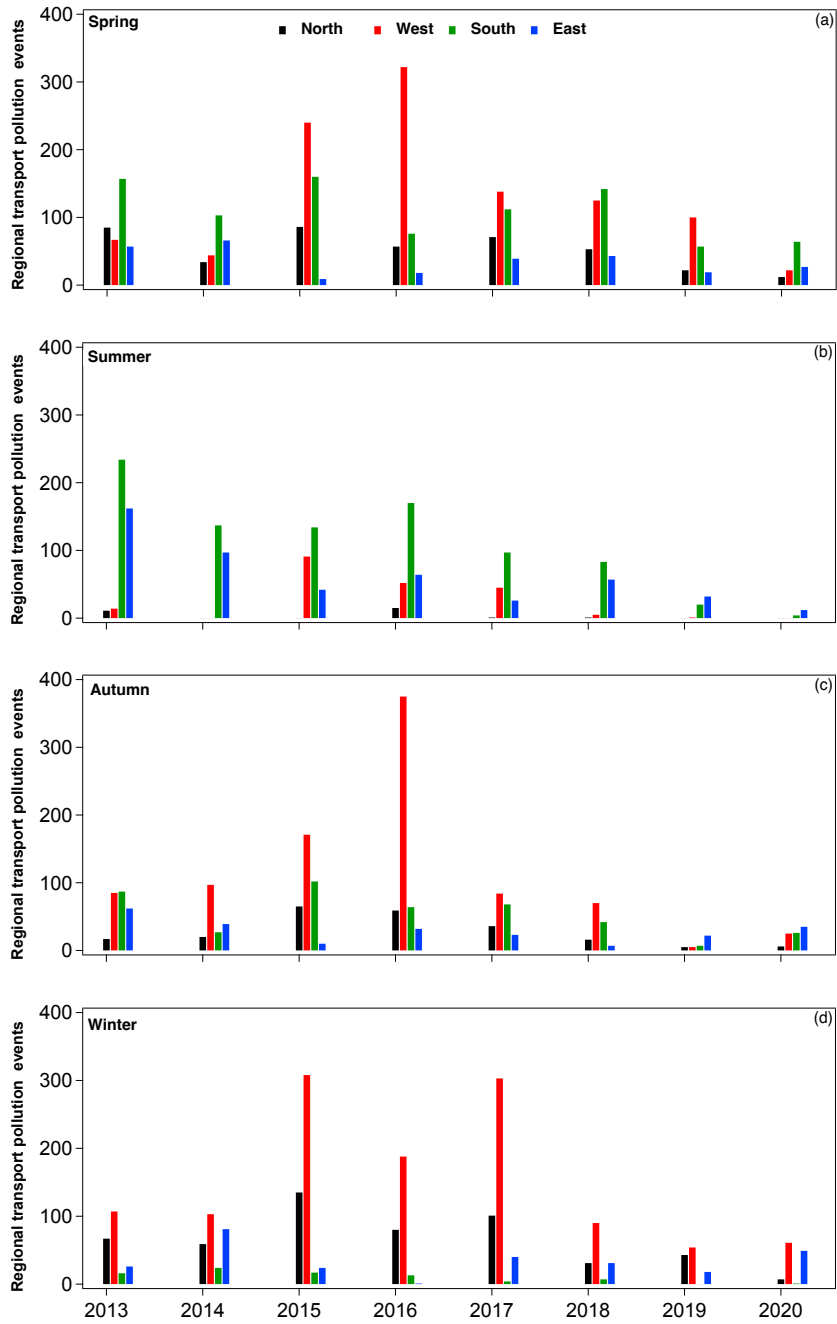
55



56

57 Fig. S5. Legend identical to that of Fig. S3, but for  $PM_{2.5}$  reductions caused by regional  
 58 transport.

59



60

61 Fig. S6. Number of regional transport pollution events in each direction from 2013 to 2020

62 during (a) spring, (b) summer, (c) autumn, and (d) winter.

63

64 Table S1. Number of pollution events caused by local emissions and regional transport in  
 65 Beijing during spring.

	2013~2017	2018~2020	2013~2020
Total	3944	1407	5351
Regional transport	1941	686	2627
Local	2003	721	2724
Regional transport / Local	0.97	0.95	0.96

66

67 Table S2. Identical legends to Table S1 but for summer.

	2013~2017	2018~2020	2013~2020
Total	3223	381	3604
Regional transport	1392	215	1607
Local	1831	166	1997
Regional transport / Local	0.76	1.3	0.8

68

69 Table S3. Identical legends to Table S1 but for autumn.

	2013~2017	2018~2020	2013~2020
Total	3906	885	4791
Regional transport	1523	266	1789
Local	2383	619	3002
Regional transport / Local	0.64	0.43	0.6

70

71 Table S4. Identical legends to Table S1 but for winter.

	2013~2017	2018~2020	2013~2020
Total	4694	1395	6089
Regional transport	1697	392	2089
Local	2997	1003	4000
Regional transport / Local	0.57	0.39	0.52